Algorithm 934: Fortran 90 Subroutines to Compute Mathieu Functions for Complex Values of the Parameter

DANILO ERRICOLO and GIUSEPPE CARLUCCIO, University of Illinois at Chicago

Software to compute angular and radial Mathieu functions is provided in the case that the parameter q is a complex variable and the independent variable x is real. After an introduction on the notation and the definitions of Mathieu functions and their related properties, Fortran 90 subroutines to compute them are described and validated with some comparisons. A sample application is also provided.

1. INTRODUCTION

Mathieu functions were introduced by Émile Léonard Mathieu in 1868 to study the vibration modes of an elliptical membrane [Mathieu 1868]. Since then, many other authors have investigated their properties and the most important results are included in McLachlan [1964], Meixner and Schäfke [1954], and Staff of the Computation Laboratory [1967]. Mathieu functions are the solutions of Mathieu's differential equation

$$\frac{d^2y}{dx^2} + (a - 2q\cos^2 x)y = 0,\tag{1}$$

which are also called angular Mathieu functions. Replacing x with ix in the previous equation yields the modified Mathieu differential equation

$$\frac{d^2y}{dx^2} - (a - 2q\cosh^2 x)y = 0,\tag{2}$$

whose solutions are called radial Mathieu functions.

Solutions of both differential equations depend upon the parameter q, which could take complex values.

The computation of Mathieu functions is not a trivial problem and software packages that compute them when q is real have been developed by, among others, Clemm [1969, 1970], Hodge [1972], Rengarajan and Lewis [1980], Frisch [1972], Baker [1992], Shirts

[1993a], [1993b], IMSL [1994], Zhang and Jin [1996], Alhargan [2001], Erricolo [2006], and Wolfram [2003]. When q is complex, Mathematica® provides solutions, but only for the angular functions. The novelty of this article is to extend to the case of complex values of q, the results presented in Erricolo [2006].

2. ANGULAR AND RADIAL OF MATHIEU FUNCTIONS

In the following, we will use the notation of Blanch and Rhodes [1955] (which is also available in National Bureau of Standards [1951], Staff of the Computation Laboratory [1967]), and Stratton [1941].

Equation (1) is periodic and in many physical applications only periodic solutions are of interest. For a given q, there exist two countable sets of values of a for which Equation (1) admits periodic solutions. These values of a are called characteristic values, and depending upon the set, the period of the solution is either π or 2π. There are four kinds of periodic solutions of (1) associated with the characteristic values a:

$$\mathrm{Se}_{2r}(q, x) = \sum_{k=0}^{\infty} \mathrm{De}_{2k}^{(2r)} \cos 2kx \qquad \text{(of period } \pi) \qquad (3)$$

$$\mathrm{Se}_{2r+1}(q, x) = \sum_{k=0}^{\infty} \mathrm{De}_{2k+1}^{(2r+1)} \cos(2k+1)x \qquad \text{(of period } 2\pi) \qquad (4)$$

$$\mathrm{So}_{2r}(q, x) = \sum_{k=1}^{\infty} \mathrm{Do}_{2k}^{(2r)} \sin 2kx \qquad \text{(of period } \pi) \qquad (5)$$

$$\mathrm{So}_{2r+1}(q, x) = \sum_{k=0}^{\infty} \mathrm{Do}_{2k+1}^{(2r+1)} \sin(2k+1)x \qquad \text{(of period } 2\pi) \qquad (6)$$

The functions $\mathrm{Se}_n(q, ix)$ and $\mathrm{So}_n(q, ix)$ clearly satisfy (2) for the same characteristic values a, but (3)–(6) converge slowly. Therefore the solutions of (2) are written in terms of rapidly converging series of products of Bessel functions associated with the same coefficients De_m, Do_m of the angular functions. Their expressions are:

$$\mathrm{Re}_{2r}^{(1)}(q, x) = \frac{(-1)^r}{\mathrm{De}_0^{(2r)}} \sqrt{\frac{\pi}{2}} \sum_{k=0}^{\infty} (-1)^k \mathrm{De}_{2k}^{(2r)} J_k(s) J_k(t), \qquad (7)$$

$$\mathrm{Re}_{2r+1}^{(1)}(q, x) = \frac{(-1)^r}{\mathrm{De}_1^{(2r+1)}} \sqrt{\frac{\pi}{2}} \sum_{k=0}^{\infty} (-1)^k \mathrm{De}_{2k+1}^{(2r+1)} [J_{k+1}(s) J_k(t) + J_k(s) J_{k+1}(t)], \qquad (8)$$

$$\mathrm{Ro}_{2r}^{(1)}(q, x) = \frac{(-1)^r}{\mathrm{Do}_2^{(2r)}} \sqrt{\frac{\pi}{2}} \sum_{k=1}^{\infty} (-1)^k \mathrm{Do}_{2k}^{(2r)} [J_{k+1}(s) J_{k-1}(t) - J_{k+1}(t) J_{k-1}(s)], \qquad (9)$$

$$\mathrm{Ro}_{2r+1}^{(1)}(q, x) = \frac{(-1)^r}{\mathrm{Do}_1^{(2r+1)}} \sqrt{\frac{\pi}{2}} \sum_{k=0}^{\infty} (-1)^k \mathrm{Do}_{2k+1}^{(2r+1)} [J_{k+1}(s) J_k(t) - J_k(s) J_{k+1}(t)], \qquad (10)$$

where

$$s = \sqrt{q} e^x, \quad t = \sqrt{q} e^{-x}. \qquad (11)$$

The radial functions of the first kind have parity either even, $\mathrm{Re}_n^{(1)}$, or odd, $\mathrm{Ro}_n^{(1)}$. A second set of solutions for the modified Mathieu equation is obtained by replacing the Bessel functions $J_m(s)$ in the previous equations with the Bessel functions $Y_m(s)$. This substitution yields the modified functions of the second kind. In many physical

applications they are referred to as radial functions of the second kind. They have parity either even, $\mathrm{Re}_n^{(2)}$, or odd, $\mathrm{Ro}_n^{(2)}$.

$$\mathrm{Re}_{2r}^{(2)}(q, x) = \frac{(-1)^r}{\mathrm{De}_0^{(2r)}} \sqrt{\frac{\pi}{2}} \sum_{k=0}^{\infty} (-1)^k \mathrm{De}_{2k}^{(2r)} Y_k(s) J_k(t), \tag{12}$$

$$\mathrm{Re}_{2r+1}^{(2)}(q, x) = \frac{(-1)^r}{\mathrm{De}_1^{(2r+1)}} \sqrt{\frac{\pi}{2}} \sum_{k=0}^{\infty} (-1)^k \mathrm{De}_{2k+1}^{(2r+1)} [Y_{k+1}(s) J_k(t) + Y_k(s) J_{k+1}(t)], \tag{13}$$

$$\mathrm{Ro}_{2r}^{(2)}(q, x) = \frac{(-1)^r}{\mathrm{Do}_2^{(2r)}} \sqrt{\frac{\pi}{2}} \sum_{k=1}^{\infty} (-1)^k \mathrm{Do}_{2k}^{(2r)} [Y_{k+1}(s) J_{k-1}(t) - Y_{k-1}(s) J_{k+1}(t)], \tag{14}$$

$$\mathrm{Ro}_{2r+1}^{(2)}(q, x) = \frac{(-1)^r}{\mathrm{Do}_1^{(2r+1)}} \sqrt{\frac{\pi}{2}} \sum_{k=0}^{\infty} (-1)^k \mathrm{Do}_{2k+1}^{(2r+1)} [Y_{k+1}(s) J_k(t) - Y_k(s) J_{k+1}(t)]. \tag{15}$$

Similar to Hankel functions, one defines modified functions of the third and fourth kinds. They are also referred to as radial functions and they have even parity

$$\mathrm{Re}_n^{(3)} = \mathrm{Re}_n^{(1)} + i \mathrm{Re}_n^{(2)}, \tag{16}$$

$$\mathrm{Re}_n^{(4)} = \mathrm{Re}_n^{(1)} - i \mathrm{Re}_n^{(2)}, \tag{17}$$

and odd parity

$$\mathrm{Ro}_n^{(3)} = \mathrm{Ro}_n^{(1)} + i \mathrm{Ro}_n^{(2)}, \tag{18}$$

$$\mathrm{Ro}_n^{(4)} = \mathrm{Ro}_n^{(1)} - i \mathrm{Ro}_n^{(2)}. \tag{19}$$

Let $a_r(q)$ be the characteristic values associated with even solutions and $b_r(q)$ those associated with odd solutions. Notice that $r = 0, 1, 2, \ldots$ and $r = 0$ applies only to a_r. The following four properties hold for complex values of q.

Property 1. When $q \to 0$, $a_r(q) \to r^2$ and $b_r(q) \to r^2$.
Property 2. $a_{2r}(-q) = a_{2r}(q)$, $b_{2r}(-q) = b_{2r}(q)$, $a_{2r+1}(-q) = b_{2r+1}(q)$.
Property 3. When q is real and not zero, the characteristic values can be ordered as
$a_0 < b_1 < a_1 < b_2 < \cdots < b_r < a_r < \cdots, q > 0$
$a_0 < a_1 < b_1 < b_2 < a_2 < a_3 < b_3 < \cdots a_{2r-1} < b_{2r-1} < b_{2r} < a_{2r} < \ldots, q < 0$.
Property 4. When q is real, the solutions associated with $a_r(q)$ and $b_r(q)$ have r zeros in $[0, \pi)$.

Properties 1 and 3 establish the ordering principle for the solutions of the Mathieu equation. Specifically, the order r of a Mathieu function is given by the position r of the characteristic value a_r (or b_r) in the sequence of characteristic values. Mathieu functions of different order are associated with different expansion coefficients De^r (Do^r), which depend on a_r (b_r), as implied by the definitions (3)–(10), (12)–(19). When coupled with the continuity of $a_r(q)$ and $b_r(q)$, Properties 1 and 3 are the only criteria available to order the characteristic values $a_r(q)$ and $b_r(q)$ in the complex plane [Blanch and Clemm 1969].

It is sufficient to know the solutions of the Mathieu equation when q belongs to the first quadrant. In fact, all values of q may be reduced to the first quadrant because of Property 2 and also because if $y(z)$ is a solution associated with a and q, then y^* is a solution associated with q^* and a^*.

3. NORMALIZATION, PROPERTIES, ORTHOGONALITY, WRONSKIAN

There exist at least three different normalizations for the Mathieu functions. In this work, we use the normalization of Stratton [1941], and accordingly, the Mathieu angular functions are normalized so that

$$\mathrm{Se}_r(q, 0) = 1, \left. \frac{d\mathrm{So}_r(q, x)}{dx} \right|_{x=0} = 1. \tag{20}$$

Therefore the expansion coefficients must satisfy

$$\sum_{k=0}^{\infty} \mathrm{De}_{2k+p}^{(r)} = 1, \sum_{k=0}^{\infty} (2k + p)\mathrm{Do}_{2k+p}^{(r)} = 1, \tag{21}$$

with $p = 0, 1$ depending on the order r. Mathieu angular functions satisfy the following orthogonality relations.

$$\int_0^{2\pi} \mathrm{Se}_m(q, x)\mathrm{Se}_n(q, x)dx = \begin{cases} 0 & m \neq n \\ N_m^e & m = n, \end{cases} \tag{22}$$

$$\int_0^{2\pi} \mathrm{So}_m(q, x)\mathrm{So}_n(q, x)dx = \begin{cases} 0 & m \neq n \\ N_m^o & m = n, \end{cases} \tag{23}$$

$$\int_0^{2\pi} \mathrm{Se}_m(q_1, x)\mathrm{So}_n(q_2, x)dx = 0, \forall m, n, q_1, q_2. \tag{24}$$

The normalization coefficients appear in the previous relations

$$N_{2r}^e = \pi \left[2\big(\mathrm{De}_0^{(2r)}\big)^2 + \big(\mathrm{De}_2^{(2r)}\big)^2 + \big(\mathrm{De}_4^{(2r)}\big)^2 + \cdots \right], \tag{25}$$

$$N_{2r+1}^e = \pi \left[\big(\mathrm{De}_1^{(2r+1)}\big)^2 + \big(\mathrm{De}_3^{(2r+1)}\big)^2 + \cdots \right], \tag{26}$$

$$N_{2r}^o = \pi \left[\big(\mathrm{Do}_2^{(2r)}\big)^2 + \big(\mathrm{Do}_4^{(2r)}\big)^2 + \cdots \right], \tag{27}$$

$$N_{2r+1}^o = \pi \left[\big(\mathrm{Do}_1^{(2r+1)}\big)^2 + \big(\mathrm{Do}_3^{(2r+1)}\big)^2 + \cdots \right]. \tag{28}$$

3.1. Relations between Solutions for the Parameter q and $-q$

The following relations hold for the angular functions

$$\mathrm{Se}_{2r}(-q, x) = \frac{\mathrm{Se}_{2r}(q, \pi/2 - x)}{\mathrm{Se}_{2r}(q, \pi/2)} \qquad \mathrm{De}_{2k}^{(2r)}(-q) = \frac{(-1)^k \mathrm{De}_{2k}^{(2r)}(q)}{\mathrm{Se}_{2r}(q, \pi/2)}, \tag{29}$$

$$\mathrm{Se}_{2r+1}(-q, x) = \frac{\mathrm{So}_{2r+1}(q, \pi/2 - x)}{\mathrm{So}_{2r+1}(q, \pi/2)} \qquad \mathrm{De}_{2k+1}^{(2r+1)}(-q) = \frac{(-1)^k \mathrm{Do}_{2k+1}^{(2r+1)}(q)}{\mathrm{So}_{2r+1}(q, \pi/2)}, \tag{30}$$

$$\mathrm{So}_{2r+1}(-q, x) = -\frac{\mathrm{Se}_{2r+1}(q, \pi/2 - x)}{\mathrm{Se}'_{2r+1}(q, \pi/2)} \qquad \mathrm{Do}_{2k+1}^{(2r+1)}(-q) = \frac{(-1)^{k+1} \mathrm{De}_{2k+1}^{(2r+1)}(q)}{\mathrm{Se}'_{2r+1}(q, \pi/2)}, \tag{31}$$

$$\mathrm{So}_{2r}(-q, x) = -\frac{\mathrm{So}_{2r}(q, \pi/2 - x)}{\mathrm{So}'_{2r}(q, \pi/2)} \qquad \mathrm{Do}_{2k}^{(2r)}(-q) = \frac{(-1)^k \mathrm{Do}_{2k}^{(2r)}(q)}{\mathrm{So}'_{2r}(q, \pi/2)}. \tag{32}$$

For the radial functions of even order

$$\mathrm{Re}_{2r}^{(1)}(-q, x) = \mathrm{Re}_{2r}^{(1)}(q, x + i\pi/2), \tag{33}$$

$$\mathrm{Re}_{2r}^{(2)}(-q, x) = \mathrm{Re}_{2r}^{(2)}(q, x + i\pi/2), \tag{34}$$

$$\mathrm{Ro}_{2r}^{(1)}(-q, x) = \mathrm{Ro}_{2r}^{(1)}(q, x + i\pi/2), \tag{35}$$

$$\mathrm{Ro}_{2r}^{(2)}(-q, x) = \mathrm{Ro}_{2r}^{(2)}(q, x + i\pi/2), \tag{36}$$

and for the radial functions of odd order

$$\mathrm{Re}_{2r+1}^{(1)}(-q, x) = \mathrm{Ro}_{2r+1}^{(1)}(q, x + i\pi/2), \tag{37}$$

$$\mathrm{Ro}_{2r+1}^{(1)}(-q, x) = \mathrm{Re}_{2r+1}^{(1)}(q, x + i\pi/2), \tag{38}$$

$$\mathrm{Re}_{2r+1}^{(2)}(-q, x) = \mathrm{Ro}_{2r+1}^{(2)}(q, x + i\pi/2), \tag{39}$$

$$\mathrm{Ro}_{2r+1}^{(2)}(-q, x) = \mathrm{Re}_{2r+1}^{(2)}(q, x + i\pi/2). \tag{40}$$

The Mathieu radial functions of argument $x + i\pi/2$ may be expressed in terms of the modified Bessel functions I and K using the following relations [Abramovitz and Stegun 1970].

$$J_m(iw) = i^m I_m(w), \qquad Y_m(iw) = i^{m+1}\left[I_m(w) + i\frac{2}{\pi}(-1)^m K_m(w)\right], \tag{41}$$

$$\cosh(w + i\pi/2) = i\sinh(w), \quad \sinh(w + i\pi/2) = i\cosh(w), \quad \tanh(w + i\pi/2) = \coth(w), \tag{42}$$

where w is a complex variable with $-\pi < \arg w \leq \pi/2$. In fact, using definition (11), when $x \to x + i\pi/2$, the argument of the Bessel functions become $s \to is$ and $t \to -it$, so that the radial functions of the first kind become

$$\mathrm{Re}_{2r}^{(1)}(-q, x) = (-1)^r\sqrt{\frac{\pi}{2}}\mathrm{Ie}_{2r}(q, x), \tag{43}$$

$$\mathrm{Re}_{2r+1}^{(1)}(-q, x) = i(-1)^r\sqrt{\frac{\pi}{2}}\mathrm{Ie}_{2r+1}(q, x), \tag{44}$$

$$\mathrm{Ro}_{2r}^{(1)}(-q, x) = (-1)^r\sqrt{\frac{\pi}{2}}\mathrm{Io}_{2r}(q, x), \tag{45}$$

$$\mathrm{Ro}_{2r+1}^{(1)}(-q, x) = i(-1)^r\sqrt{\frac{\pi}{2}}\mathrm{Io}_{2r+1}(q, x), \tag{46}$$

where

$$\mathrm{Ie}_{2r}(q, x) = \sum_{k=0}^{\infty}(-1)^k\mathrm{De}_{2k}^{(2r)}(q)I_k(s)I_k(t)\big/\mathrm{De}_0^{(2r)}(q), \tag{47}$$

$$\mathrm{Ie}_{2r+1}(q, x) = \sum_{k=0}^{\infty}(-1)^k\mathrm{Do}_{2k+1}^{(2r+1)}(q)[I_{k+1}(s)I_k(t) + I_{k+1}(t)I_k(s)]\big/\mathrm{Do}_1^{(2r+1)}(q), \tag{48}$$

$$\mathrm{Io}_{2r}(q, x) = \sum_{k=1}^{\infty}(-1)^k\mathrm{Do}_{2k}^{(2r)}(q)[I_{k-1}(s)I_{k+1}(t) - I_{k+1}(s)I_{k-1}(t)]\big/\mathrm{Do}_2^{(2r)}(q), \tag{49}$$

$$\mathrm{Io}_{2r+1}(q, x) = \sum_{k=0}^{\infty}(-1)^k\mathrm{De}_{2k+1}^{(2r+1)}(q)[I_{k+1}(s)I_k(t) - I_k(t)I_{k+1}(s)]\big/\mathrm{De}_1^{(2r+1)}(q). \tag{50}$$

The radial functions of the second kind are complex for real value of x, yielding

$$\mathrm{Re}_{2r}^{(2)}(-q,x) = (-1)^r \left[i\sqrt{\pi/2}\,\mathrm{Ie}_{2r}(q,x) - \sqrt{\frac{2}{\pi}}\,\mathrm{Ke}_{2r}(q,x) \right], \tag{51}$$

$$\mathrm{Re}_{2r+1}^{(2)}(-q,x) = (-1)^r \left[-\sqrt{\pi/2}\,\mathrm{Ie}_{2r+1}(q,x) + i\sqrt{\frac{2}{\pi}}\,\mathrm{Ke}_{2r+1}(q,x) \right], \tag{52}$$

$$\mathrm{Ro}_{2r}^{(2)}(-q,x) = (-1)^r \left[i\sqrt{\pi/2}\,\mathrm{Io}_{2r}(q,x) - \sqrt{\frac{2}{\pi}}\,\mathrm{Ko}_{2r}(q,x) \right], \tag{53}$$

$$\mathrm{Ro}_{2r+1}^{(2)}(-q,x) = (-1)^r \left[-\sqrt{\pi/2}\,\mathrm{Io}_{2r+1}(q,x) + i\sqrt{\frac{2}{\pi}}\,\mathrm{Ko}_{2r+1}(q,x) \right], \tag{54}$$

where

$$\mathrm{Ke}_{2r}(q,x) = \sum_{k=0}^{\infty} \mathrm{De}_{2k}^{(2r)}(q) I_k(t) K_k(s) \big/ \mathrm{De}_0^{(2r)}(q), \tag{55}$$

$$\mathrm{Ke}_{2r+1}(q,x) = \sum_{k=0}^{\infty} \mathrm{Do}_{2k+1}^{(2r+1)}(q)[I_k(t)K_{k+1}(s) - I_{k+1}(t)K_k(s)] \big/ \mathrm{Do}_1^{(2r+1)}(q), \tag{56}$$

$$\mathrm{Ko}_{2r}(q,x) = \sum_{k=0}^{\infty} \mathrm{Do}_{2k}^{(2r)}(q)[I_{k-1}(t)K_{k+1}(s) - I_{k+1}(t)K_{k-1}(s)] \big/ \mathrm{Do}_2^{(2r)}(q), \tag{57}$$

$$\mathrm{Ko}_{2r+1}(q,x) = \sum_{k=0}^{\infty} \mathrm{De}_{2k+1}^{(2r)}(q)[I_{k+1}(t)K_k(s) + I_k(t)K_{k+1}(s)] \big/ \mathrm{De}_1^{(2r)}(q). \tag{58}$$

4. COMPUTATION OF MATHIEU FUNCTIONS

Mathieu functions are computed according to the following three main steps: (1) computation of the characteristic values; (2) computation of the expansion coefficients De_m or Do_m; and, (3) evaluation of the series expansions (3)–(10), (12)–(19).

4.1. Computation of the Characteristic Values

The Mathieu characteristic values depend on the parameter q, the parity of the Mathieu function and its order n. One approach to compute them is to solve an eigenvalue problem that leads to an infinite set of eigenvalues that approximate the characteristic values a_r (b_r) associated with the parameter q.

When q is real, the characteristic values are real and it is possible to sort them according to Property 3. This sorting provides the rule to determine the order n of the Mathieu function. Specifically, the solution of order n is the one generated using the characteristic value at position n in the sorted sequence. However, when q is not real, the characteristic values are complex and they cannot be sorted, which prevents a direct association between a specific characteristic value and its corresponding Mathieu function.

Fortunately, the continuity of the characteristic values $a_r(q)$ and $b_r(q)$ provides a method to determine the appropriate characteristic value to generate a requested Mathieu function of order n, which is explained next.

4.1.1. Tracking algorithm. Assume that $q = q_{\mathrm{real}} + iq_{\mathrm{imag}}$ and that the parity and order of the Mathieu function are given. The following algorithm determines the appropriate

characteristic value, $a_r(q_{\text{temp}})$ or $b_r(q_{\text{temp}})$, when $q_{\text{temp}} = q_{\text{real}}$, and then tracks the characteristic value as q_{temp} is changed until it reaches $q_{\text{temp}} = q$.

Step 1. Let $q_0 = q_{\text{real}}$, and compute the characteristic values associated with q_0. The characteristic values are the eigenvalues of an infinite matrix whose entries depend on q, n, and on the parity of the Mathieu function. Since q_0 is real, the eigenvalues of the matrix are real and can be sorted. The infinite matrix is truncated to an order $N > n$, which is sufficiently large, $(N = 10 + 2n)$, so that the first n eigenvalues of the truncated matrix are good approximations of the first n characteristic values. Each characteristic value a_r^0 (b_r^0) is associated with the eigenvalue at position r in the sequence, and the one at the location $r = n$ is selected. This is performed by `initial_eigenvalue_approximation`.

Step 2 Consider an increment Δq_{imag} so that $\Delta q_{\text{imag}} \leq 0.5$, and set $p = 0$.

Step 3 Let $p = p + 1$, $q_{\text{temp}}^p = q_0 + ip\Delta q_{\text{imag}}$. Then use the method described in Blanch [1966] to refine the characteristic value $a_n^p(q_{\text{temp}}^p)$, using as initial approximation $a_n^{p-1}(q_{\text{temp}}^{p-1})$.

Step 4 If $q_{\text{temp}^p} \neq q$ then go back to Step 3, otherwise the last value found for a_n^p (b_n^p) is the characteristic value of order n associated with q.

Steps 3 and 4 are both performed by `Mathieu_Eigenvalue_and_Coefficients`.

This software could be extended to allow for the simultaneous computation of all Mathieu functions of order below the maximum order n. This extension requires the simultaneous computation of all the characteristic values $a_r(q)$ or $b_r(q)$, $r = 0, \ldots, n$, and could be accomplished with the following variation of the tracking algorithm. At Step 3, instead of using Blanch's algorithm, one could replace it with the following.

Step 3. Let $p = p + 1$, $q_{\text{temp}}^p = q_0 + ip\Delta q_{\text{imag}}$. Create a new truncated matrix, similar to Step 1, for the parameter q_{temp}^p and compute its eigenvalues e_ℓ, $\ell = 1, \ldots, N$. Let $d_{\ell s}$ be the distance between the eigenvalue e_ℓ and the previous characteristic value approximation $a_s^{p-1}(q_{\text{temp}}^{p-1})$ or $b_s^{p-1}(q_{\text{temp}}^{p-1})$. For each $s = 1, \ldots, n$, compute all distances $d_{\ell s}$. The characteristic value $a_s^p(q_{\text{temp}}^p)$ or $b_s^p(q_{\text{temp}}^p)$ is the eigenvalue e_ℓ for which the distance $d_{\ell s}$ is minimal.

4.2. Computation of the Expansion Coefficients

The expansion coefficients De_m (Do_m) are computed using four recurrence relations obtained by substituting the series expansion for the angular functions (3)–(6) into Mathieu Differential Equation (1).

Blanch [1966] showed that each relation may be written as both a forward or a backward recurrence for any characteristic value a_r (b_r). In particular, she found the property that when the value of a_r (b_r) is the characteristic value then both the forward and the backward recurrence relations produce the same expansion coefficients. This property is also used at Steps 3 and 4 of the previous section to refine the value computed for a_r (b_r), by computing appropriate derivatives of a_r (b_r) and using them in a Newton scheme to improve the initial value of a_r (b_r). Once the value of a_r (b_r) has been determined, the expansion coefficients are computed using both the forward and the backward recurrence relations by the subroutine `Mathieu_Eigenvalue_and_Coefficients`.

In the computation of the expansion coefficients, it is sufficient to consider values of the parameter q such that $\text{real}(q) \geq 0$ because of the relations between Mathieu functions for the parameter q and $-q$ presented in Section 3.1.

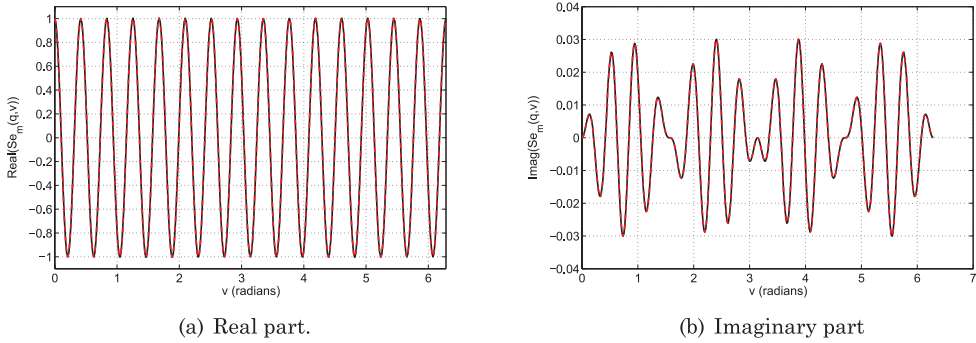(a) Real part.   (b) Imaginary part

Fig. 1. Plot of $Se_m(q, v)$ for $m = 15$ and $q = -0.9 + i0.9$. Fortran results are indicated with a solid black line, while power series MATLAB® results are indicated with a dashed red line. The two curves overlap.

4.3. Evaluation of the Series Expansions

4.3.1. Angular Functions. Mathieu angular functions are computed using the series expansions (3)–(6) by the function `MathieuAngular` for real values of the variable x and complex values of the parameter q. When x takes complex values, the appropriate function call is `MathieuAngular_cmplx`.

4.3.2. Radial Functions. Mathieu radial functions are computed using the series expansions (7)–(10), (12)–(19) by the function `MathieuRadial`, which accepts real values of the variable x and complex values of the parameter q.

Specifically, the function `MathieuRadial` operates in the following way. When $real(q) \geq 0$, it applies the tracking algorithm, it determines the expansion coefficients, and computes the appropriate series expansions using the definitions (7)–(10), (12)–(19). When $real(q) \leq 0$, it introduces a temporary variable $q1 = -q$ and performs the same steps as for the previous case, where $q1$ replaces q. Then, the radial functions are obtained by applying the relations given in Section 3.1.

5. VALIDATION

These subroutines have been validated by making comparisons as described in the following.

—When $|q|$ is sufficiently small, comparisons can be made with the McLaurin expansions of the Mathieu functions described in Larsen et al. [2008].
—By comparison with Mathematica®.
—Another check is obtained by controlling the Wronskian value.

In the following, u is the argument of the angular Mathieu function and v is the argument of the radial Mathieu function because of the physical meaning of u and v, which is related to the transformation from elliptic cylinder to rectangular Cartesian coordinates given in Equation (62) as part of the sample application given in Section 6.

5.1. Comparison with Power Series

We compare our results to the values obtained by using the small argument series expansion approximation [Larsen et al. 2008] of the solutions calculated by a subroutine programmed in MATLAB®. Figure 1 shows the results of the comparison in the case of the even angular Mathieu function $Se_m(q, v)$ for $m = 15$ and $q = -0.9 + i0.9$. Figure 2 shows the results of the comparison in the case of the odd angular Mathieu function $So_m(q, v)$ for $m = 10$ and $q = -0.9 + i0.9$.
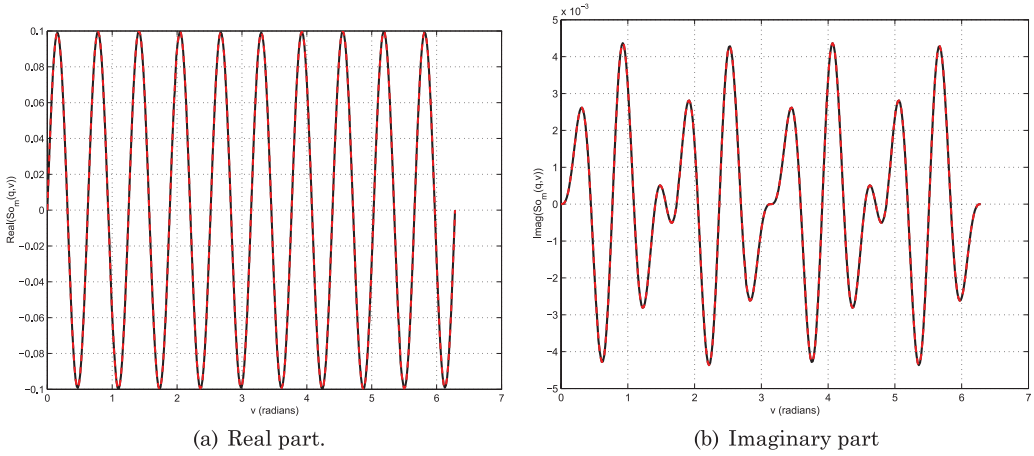
Fig. 2.   Plot of $So_m(q, v)$ for $m = 10$ and $q = -0.9 + i0.9$. Fortran results are indicated with a solid black line, while power series MATLAB® results are indicated with a dashed red line. The two curves overlap.

Fig. 3.   Plot of $Re_m^{(1)}$ for $m = 5$ and $q = -0.8 + i0.7$. Fortran results are indicated with a solid black line, while power series MATLAB® results are indicated with a dashed red line. The two curves overlap.

Figure 3 shows the results of the comparison in the case even radial Mathieu functions of the first kind $Re_m^{(1)}(q, u)$ for $m = 5$ and $q = -0.8 + i0.7$. Figure 4 shows the results of the comparison in the case of even radial Mathieu functions of the second kind, $Re_m^{(2)}(q, u)$ for $m = 5$ and $q = -0.8 + i0.7$. Figure 5 shows the results of the comparison in the case of odd radial Mathieu functions of the first kind $Ro_m^{(1)}(q, u)$, for $m = 3$ and $q = 0.2025 + i0.5$. Figure 6 shows the results of the comparison in the case of even radial Mathieu functions of the second kind $Ro_m^{(2)}(q, u)$, for $m = 3$ and $q = 0.2025 + i0.5$. Next we show the comparisons with the small argument power series as a function of q. In Figure 7, the angular Mathieu function $Se_m(q, v)$ is evaluated for $m = 1$, $v = 1$, and $q = q_r + iq_i$, with $q_i = 0.5$, while $-0.5 < q_r < 0.5$. In Figure 8, the even radial Mathieu function of the first kind $Re_m^1(q, u)$ is evaluated for $m = 1$, $u = 1$, and $q = q_r + iq_i$, with $q_i = 0.5$, while $-0.5 < q_r < 0.5$. In both cases, there is good agreement between the Fortran results and the small argument power expansion.

(a) Real part.   (b) Imaginary part

Fig. 4.   Plot of $\mathrm{Re}_m^{(2)}(q, u)$ for $m = 5$ and $q = -0.8 + i0.7$. Fortran results are indicated with a solid black line, while power series MATLAB® results are indicated with a dashed red line. The two curves overlap.
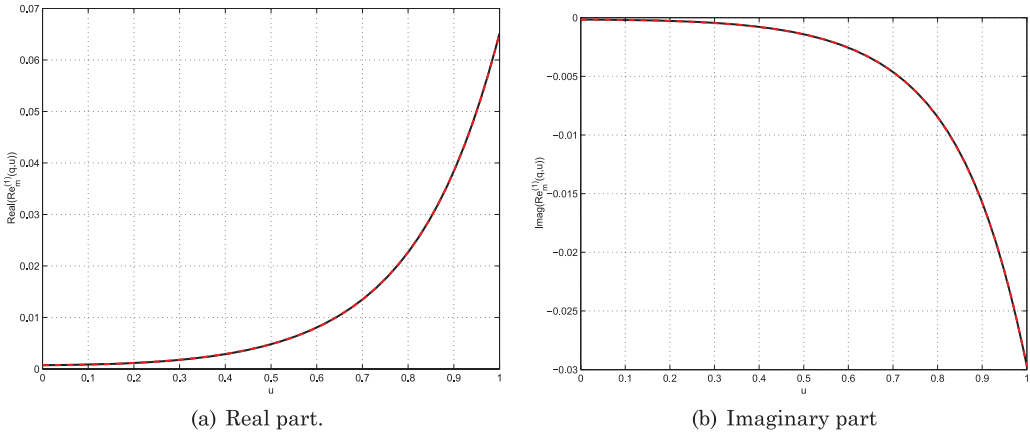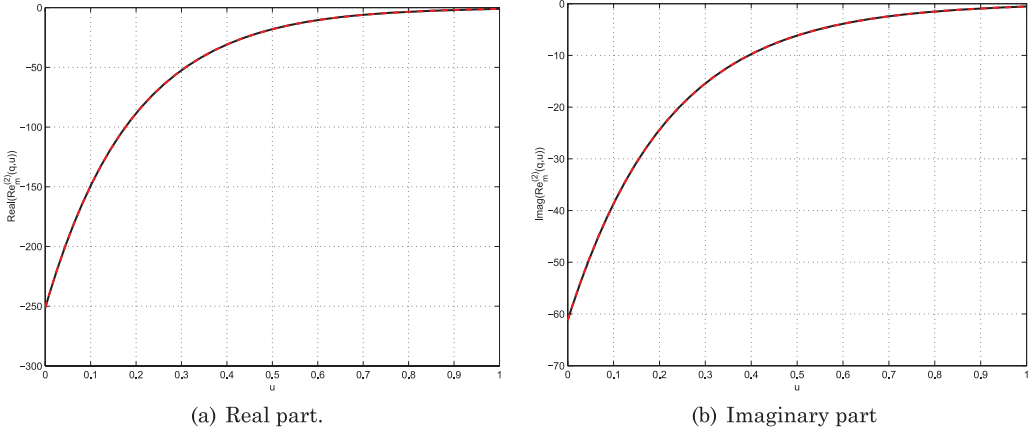

(a) Real part.   (b) Imaginary part
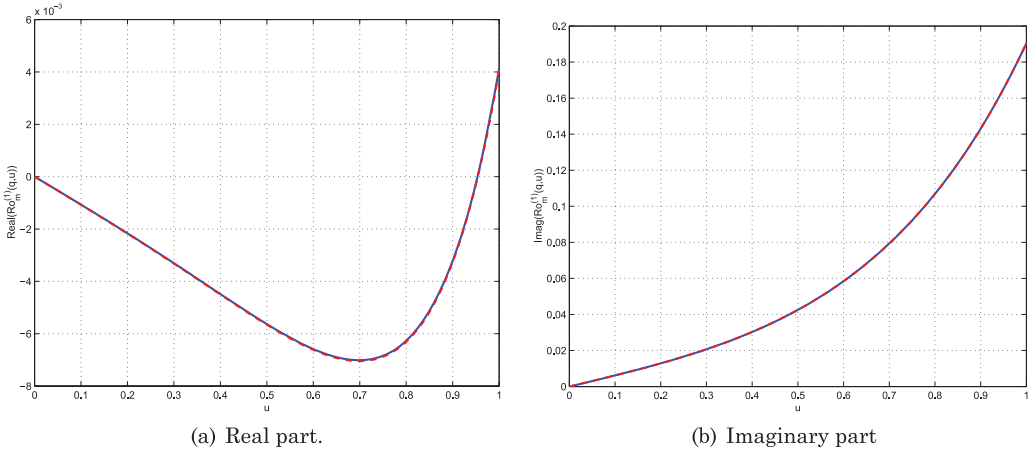
Fig. 5.   Plot of $\mathrm{Ro}_m^{(1)}(q, u)$ for $m = 3$ and $q = 0.2025 + i0.5$. Fortran results are indicated with a solid black line, while power series MATLAB® results are indicated with a dashed red line. The two curves overlap.

5.2. Comparison with Mathematica®

For larger values of $|q|$, Mathieu angular functions are evaluated using Mathematica® and compared to the results obtained by our subroutines. The comparison with Mathematica® is limited to the angular Mathieu functions, since there are no Mathematica® functions that compute radial Mathieu functions.

Angular Mathieu functions are evaluated in three steps: (1) given a small parameter q and order n, the Mathieu characteristic values a_r and b_r are computed using the Mathematica® functions `MathieuCharacteristicA[m,q]` and `MathieuCharacteristicB[m,q]`; (2) even angular Mathieu functions are computed using the function `MathieuC[ar,q,v]` and odd angular Mathieu functions are computed using `MathieuS[br,q,v]`; (3) the results are normalized according to Stratton:

$$\mathrm{Se}_m(q, v) = \frac{ce_m(q, v)}{ce_m(q, 0)}, \quad \mathrm{So}_m(q, v) = \frac{se_m(q, v)}{se'_m(q, 0)}, \tag{59}$$

where $se'_m(q, 0)$ is computed using the function `MathieuSPrime[br,q,v]` [Erricolo 2003].

(a) Real part.   (b) Imaginary part

Fig. 6. Plot of $\mathrm{Ro}_m^{(2)}(q, u)$ for $m = 3$ and $q = 0.2025 + i0.5$. Fortran results are indicated with a solid black line, while power series MATLAB® results are indicated with a dashed red line. The two curves overlap.
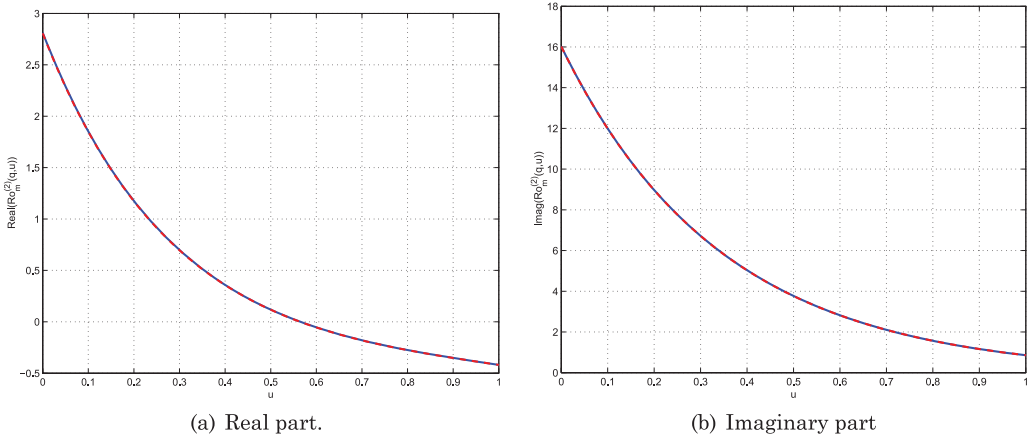

(a) Real part.   (b) Imaginary part

Fig. 7. Plot of $\mathrm{Se}_m(q, v)$ for $m = 1$, $v = 1$, while the real part of $q = q_r + iq_i$ is varied with $q_i = 0.5$. Fortran results are indicated with a solid black line, while power series MATLAB® results are indicated with a dashed red line. The two curves overlap.

(a) Real part.   (b) Imaginary part
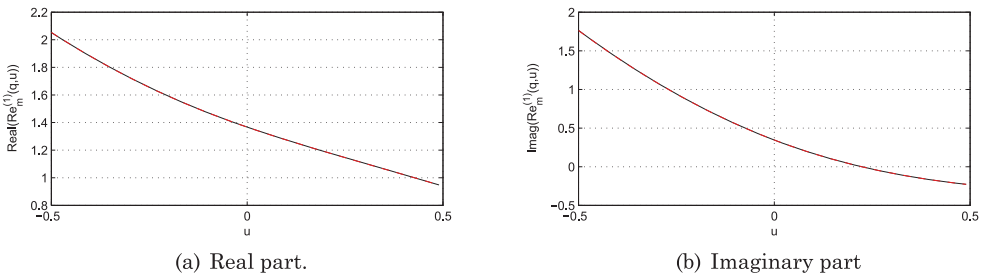
Fig. 8. Plot of $\mathrm{Re}_m(q, u)$ for $m = 1$, $u = 1$, while the real part of $q = q_r + iq_i$ is varied with $q_i = 0.5$. Fortran results are indicated with a solid black line, while power series MATLAB® results are indicated with a dashed red line. The two curves overlap.

Even angular functions $\mathrm{Se}_m(q, v)$ are examined for $m = 15$, $q = 3 + 2j$ in Figure 9(a) and Figure 9(b) by comparing the real and imaginary parts, respectively.

Odd angular functions $\mathrm{So}_m(q, v)$ are examined for $m = 10$, $q = 4 + 2j$ in Figure 10(a) and Figure 10(b) by comparing the real and imaginary parts, respectively.

It is clear from the plots that the Fortran subroutines are very accurate in calculating angular functions for small values of the parameter.

(a) Real part.

(b) Imaginary part.
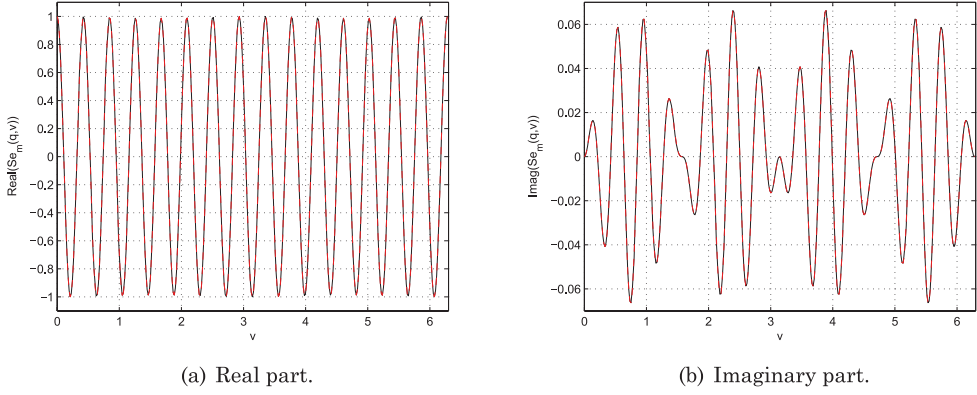
Fig. 9. Comparisons between Fortran subroutines and Mathematica® in the case of the even angular function $Se_m(q, v)$, when $m = 15$ and $q = 3 + 2i$. Fortran results are indicated with a solid black line, while Mathematica® results are indicated with a dashed red line. The two curves overlap.

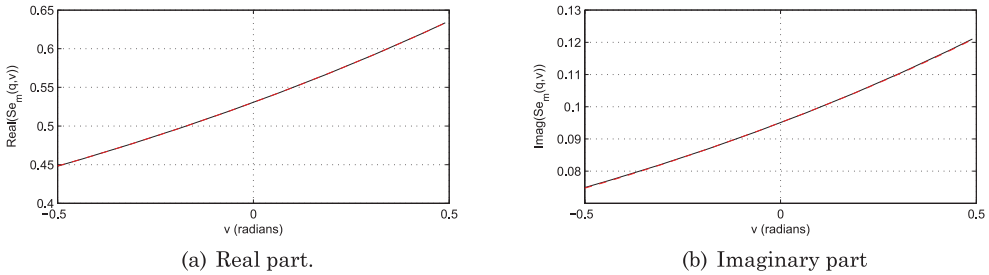(a) Real part.

(b) Imaginary part.
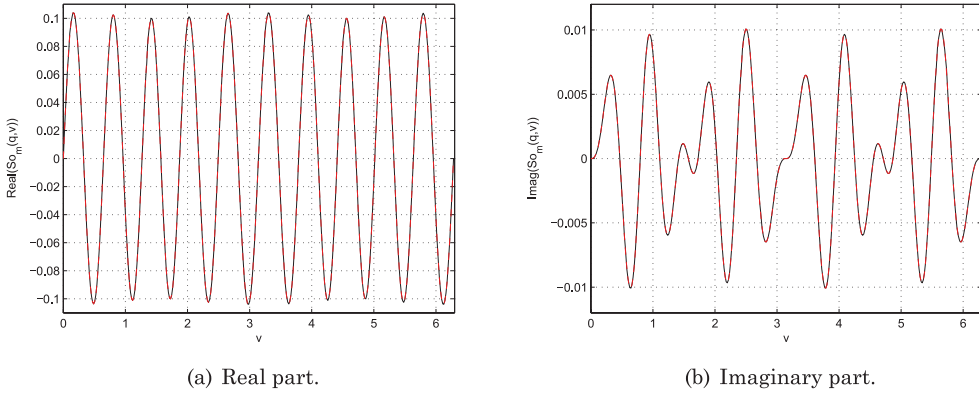
Fig. 10. Comparisons between Fortran subroutines and Mathematica® in the case of the odd angular function $So_m(q, v)$, when $m = 10$ and $q = 4 + 2j$. Fortran results are indicated with a solid black line, while Mathematica® results are indicated with a dashed red line. The two curves overlap.

## 5.3. Wronskian Check

Another way to check the accuracy of the computation of radial functions is to examine their Wronskian. This test is based on the Wronskian property

$$W_e = \text{Re}_m^{(1)}(q, u)\text{Re}_m^{(2')}(q, u) - \text{Re}_m^{(2)}(q, u)\text{Re}_m^{(1')}(q, u) = 1 \tag{60}$$

$$W_o = \text{Ro}_m^{(1)}(q, u)\text{Ro}_m^{(2')}(q, u) - \text{Ro}_m^{(2)}(q, u)\text{Ro}_m^{(1')}(q, u) = 1, \tag{61}$$

where the prime symbol refers to the derivative with respect to argument u. Table I shows the results of this test when $q = -0.9 + j0.9$ and $u = 2$. Table II shows the results of this test when $q = 2.5 + j1.8$ and $u = 2$.

Tables I and II are computed using the version of our subroutines that employs the IMSL numerical subroutines to evaluate Bessel functions and obtain the initial characteristic values a_r^0 (b_r^0). Since IMSL numerical subroutines may not be available to everyone, the software associated with this article contains other Fortran libraries to compute the Bessel functions [Amos 1986] and the eigenvalues. We would like to point out that higher accuracy is achieved when IMSL subroutines are used.

Table I. Wronskian Test for $q = -0.9 + j0.9$ and $u = 2$

n	real$(W_e - 1)$	imag(W_e)	real$(W_o - 1)$	imag(W_o)
0	$-0.497676E\text{-}07$	$-0.104774E\text{-}07$		
1	$0.582077E\text{-}10$	$0.000000E\text{+}00$	$-0.145519E\text{-}10$	$0.000000E\text{+}00$
2	$-0.203727E\text{-}09$	$0.232831E\text{-}09$	$0.000000E\text{+}00$	$0.000000E\text{+}00$
3	$0.000000E\text{+}00$	$0.000000E\text{+}00$	$-0.291038E\text{-}10$	$0.000000E\text{+}00$
4	$0.756700E\text{-}09$	$-0.631553E\text{-}08$	$0.151049E\text{-}07$	$0.321306E\text{-}07$
5	$0.538421E\text{-}09$	$-0.258660E\text{-}08$	$0.698492E\text{-}09$	$-0.217915E\text{-}08$
6	$-0.625732E\text{-}09$	$0.894943E\text{-}09$	$0.298314E\text{-}09$	$-0.107138E\text{-}08$
7	$-0.483851E\text{-}09$	$0.605269E\text{-}09$	$-0.471118E\text{-}09$	$0.537057E\text{-}09$
8	$0.647105E\text{-}09$	$-0.112777E\text{-}09$	$-0.369027E\text{-}09$	$0.383125E\text{-}09$
9	$0.696215E\text{-}09$	$-0.852083E\text{-}10$	$0.655563E\text{-}09$	$-0.596287E\text{-}10$
10	$-0.106102E\text{-}08$	$-0.669896E\text{-}09$	$0.688974E\text{-}09$	$-0.345644E\text{-}10$
11	$-0.138795E\text{-}08$	$-0.100460E\text{-}08$	$-0.129301E\text{-}08$	$-0.978877E\text{-}09$
12	$0.119574E\text{-}08$	$0.515956E\text{-}08$	$-0.162720E\text{-}08$	$-0.136690E\text{-}08$
13	$0.147028E\text{-}08$	$0.851756E\text{-}08$	$0.125216E\text{-}08$	$0.811601E\text{-}08$
14	$0.224559E\text{-}07$	$-0.356762E\text{-}07$	$0.123325E\text{-}08$	$0.124891E\text{-}07$
15	$0.441156E\text{-}07$	$-0.586881E\text{-}07$	$0.426029E\text{-}07$	$-0.535508E\text{-}07$
16	$-0.530413E\text{-}06$	$0.677142E\text{-}07$	$0.859084E\text{-}07$	$-0.964482E\text{-}07$
17	$-0.919311E\text{-}06$	$0.312372E\text{-}06$	$-0.878474E\text{-}06$	$0.138578E\text{-}06$
18	$0.875018E\text{-}05$	$0.841740E\text{-}05$	$-0.245003E\text{-}05$	$0.366472E\text{-}07$
19	$0.275663E\text{-}04$	$0.256637E\text{-}04$	$0.356364E\text{-}04$	$0.243828E\text{-}04$
20	$-0.324346E\text{-}03$	$-0.298998E\text{-}05$	$0.566832E\text{-}04$	$-0.444547E\text{-}04$

Table II. Wronskian Test for $q = 2.5 + j1.8$ and $u = 2$

n	real$(W_e - 1)$	imag(W_e)	real$(W_o - 1)$	imag(W_o)
0	$0.153153E\text{-}08$	$0.375110E\text{-}09$		
1	$0.122702E\text{-}08$	$-0.992827E\text{-}09$	$0.483169E\text{-}11$	$0.964064E\text{-}10$
2	$-0.105049E\text{-}07$	$-0.793534E\text{-}09$	$-0.142109E\text{-}11$	$0.583213E\text{-}10$
3	$-0.110762E\text{-}07$	$0.100954E\text{-}09$	$0.852651E\text{-}13$	$0.227374E\text{-}12$
4	$0.833893E\text{-}10$	$-0.295699E\text{-}09$	$-0.238742E\text{-}11$	$-0.454747E\text{-}12$
5	$0.170530E\text{-}12$	$0.248690E\text{-}12$	$0.113687E\text{-}12$	$0.568434E\text{-}13$
6	$-0.476831E\text{-}09$	$-0.367226E\text{-}08$	$0.290066E\text{-}08$	$0.727772E\text{-}08$
7	$-0.598845E\text{-}10$	$-0.171605E\text{-}08$	$0.107889E\text{-}09$	$-0.176777E\text{-}08$
8	$-0.641023E\text{-}09$	$-0.612374E\text{-}09$	$0.253621E\text{-}09$	$-0.876405E\text{-}09$
9	$-0.464766E\text{-}09$	$-0.531671E\text{-}09$	$-0.446349E\text{-}09$	$-0.581082E\text{-}09$
10	$-0.378250E\text{-}09$	$0.373390E\text{-}10$	$-0.281403E\text{-}09$	$-0.498641E\text{-}09$
11	$-0.435564E\text{-}09$	$-0.457980E\text{-}10$	$-0.441648E\text{-}09$	$-0.713598E\text{-}10$
12	$-0.236587E\text{-}09$	$0.336847E\text{-}09$	$-0.453785E\text{-}09$	$-0.181238E\text{-}09$
13	$-0.478929E\text{-}09$	$0.334858E\text{-}09$	$-0.496685E\text{-}09$	$0.315323E\text{-}09$
14	$-0.282224E\text{-}10$	$0.923046E\text{-}09$	$-0.796111E\text{-}09$	$0.188488E\text{-}09$
15	$-0.672772E\text{-}09$	$0.141019E\text{-}08$	$-0.722514E\text{-}09$	$0.138122E\text{-}08$
16	$0.130262E\text{-}08$	$0.345546E\text{-}08$	$-0.202385E\text{-}08$	$0.173100E\text{-}08$
17	$-0.465085E\text{-}09$	$0.750809E\text{-}08$	$-0.679129E\text{-}09$	$0.742430E\text{-}08$
18	$0.160675E\text{-}07$	$0.199750E\text{-}07$	$-0.673906E\text{-}08$	$0.137299E\text{-}07$
19	$0.165958E\text{-}07$	$0.583738E\text{-}07$	$0.157591E\text{-}07$	$0.580741E\text{-}07$
20	$0.226897E\text{-}06$	$0.157335E\text{-}06$	$-0.941438E\text{-}08$	$0.142480E\text{-}06$

(a) Problem geometry.   (b) Point-matching.
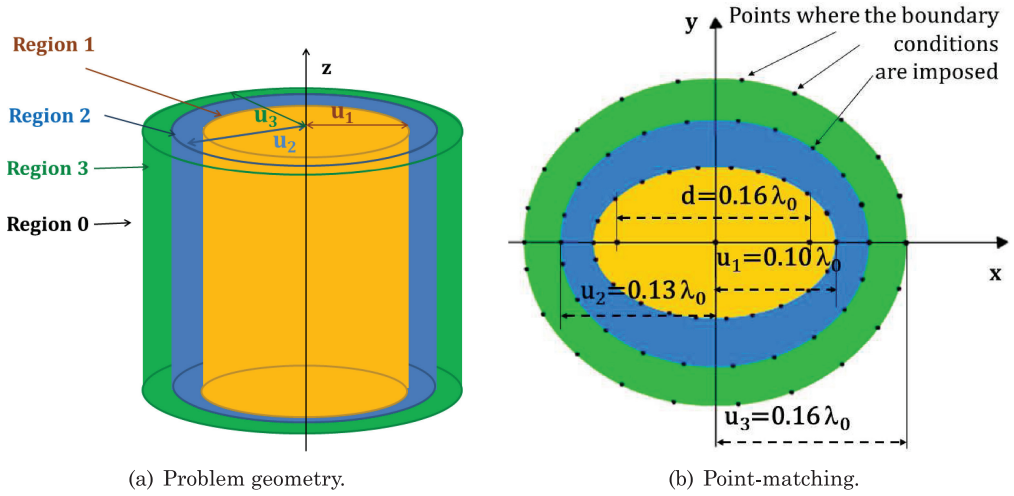
Fig. 11.   Sample problem.

6. SAMPLE APPLICATION

Mathieu functions are frequently applied in problems involving elliptical cylinder coordinates [Caorsi et al. 1997, 1998, 1999a, 1999b; Erricolo et al. 2005b, 2005a; Berardi et al. 2004; Erricolo and Uslenghi 2005b, 2004; Erricolo et al. 2006, 2008; Erricolo and Uslenghi 2005a; Valentino and Erricolo 2006, 2007; Canta and Erricolo 2008; Olshansky and Turkel 2008; Akgol et al. 2011b, 2011a, 2011; Gupta et al. 2008; Baktur et al. 2010; Bakker and Kuhlman 2011; Gil et al. 2011]. As a sample application of the Mathieu functions, we consider the two-dimensional problem of the computation of the electromagnetic field distribution inside an infinitely long lossy elliptic cylinder made of three layers, as shown in Figure 11(a), when the structure is illuminated by an incident time-harmonic plane wave. The time factor dependence $e^{i\omega t}$ is assumed and neglected throughout.

Without any loss of generality, we select a coordinate system where the z axis is the axis of the cylinder and the x and y axes correspond to the axes of symmetry of the elliptic cross section. For this geometry, it is possible to express the solution in terms of series expansions of Mathieu functions. Accordingly, we select an elliptic cylinder coordinate system [Stratton 1941; Moon and Spencer 1961], (u, v, z) with focal distance d, having two foci located along the x axis at $\pm d/2$. The elliptic cylinder coordinates (u, v, z) and the Cartesian coordinates (x, y, z) are related by

$$x = \frac{d}{2} \cosh u \cos v$$
$$y = \frac{d}{2} \sinh u \sin v \qquad\qquad (62)$$
$$z = z$$

From the previous definition, surfaces having $u = $ constant represent families of confocal elliptic cylinders, while surfaces having $v = $ constant represent families of confocal hyperbolic cylinders. There are four regions in Figure 11(a): region 1, located inside the surface $u = u_1$; region 2, limited between the surface $u = u_2$ and the surface $u = u_1$; region 3, limited between the surface $u = u_3$ and the surface $u = u_2$; and region 0, which is external to the surface $u = u_3$.

The source of the electromagnetic field is a plane wave, whose direction of propagation lies in the xy plane and makes the angle ϕ_0 with the negative x axis, and polarized with the electric field along the z direction:

$$E_z^i = E_0 e^{ik_0(x\cos\phi_0 + y\sin\phi_0)}. \tag{63}$$

The main steps that lead to the exact electromagnetic solution of this problem are briefly summarized in the following.

We first express the z component of the electric field in each region as a series expansion containing Mathieu functions [Stratton 1941; McLachlan 1964]. In doing so, we assume that each region is filled with a medium that is linear, uniform, and isotropic. The wavevector in region ℓ is k_ℓ. The z components of the electric fields in regions 1, 2, and 3 are given by Bowman et al. [1987]

$$E_{1,z} = \sum_{m=0}^{+\infty} e_{1,m}\text{Re}_m^{(1)}(q_1, u)\text{Se}_m(q_1, v) + \sum_{m=1}^{+\infty} f_{1,m}\text{Ro}_m^{(1)}(q_1, u)\text{So}_m(q_1, v), \tag{64}$$

$$E_{2,z} = \sum_{m=0}^{+\infty} \left[e_{2,m}\text{Re}_m^{(1)}(q_2, u)\text{Se}_m(q_2, v) + f_{2,m}\text{Re}_m^{(2)}(q_2, u)\text{Se}_m(q_2, v) \right]$$
$$+ \sum_{m=1}^{+\infty} \left[g_{2,m}\text{Ro}_m^{(1)}(q_2, u)\text{So}_m(q_2, v) + h_{2,m}\text{Ro}_m^{(2)}(q_2, u)\text{So}_m(q_2, v) \right], \tag{65}$$

$$E_{3,z} = \sum_{m=0}^{+\infty} \left[e_{3,m}\text{Re}_m^{(1)}(q_3, u)\text{Se}_m(q_3, v) + f_{3,m}\text{Re}_m^{(2)}(q_3, u)\text{Se}_m(q_3, v) \right]$$
$$+ \sum_{m=1}^{+\infty} \left[g_{3,m}\text{Ro}_m^{(1)}(q_3, u)\text{So}_m(q_3, v) + h_{3,m}\text{Ro}_m^{(2)}(q_3, u)\text{So}_m(q_3, v) \right], \tag{66}$$

respectively. In region 0, external to the elliptic cylinder, the electric field is given by the sum of the incident field E_z^i (63) which can be expanded in terms of Mathieu functions

$$E_z^i = \sqrt{8\pi} \left[\sum_{m=0}^{+\infty} \frac{i^m}{N_m^e} \text{Re}_m^{(1)}(q_0, u)\text{Se}_m(q_0, v)\text{Se}_m(q_0, \phi_0) \right.$$
$$\left. + \sum_{m=1}^{+\infty} \frac{i^m}{N_m^o} \text{Ro}_m^{(1)}(q_0, u)\text{So}_m(q_0, v)\text{So}_m(q_0, \phi_0) \right], \tag{67}$$

and the scattered field

$$E_{0,z} = \sum_{m=0}^{+\infty} e_{0,m}\text{Re}_m^{(4)}(q_0, u)\text{Se}_m(q_0, v) + \sum_{m=1}^{+\infty} f_{0,m}\text{Ro}_m^{(4)}(q_0, u)\text{So}_m(q_0, v), \tag{68}$$

where radial Mathieu functions of the fourth kind are used to satisfy the Sommerfeld radiation condition and $q_\ell = (k_\ell d)^2/16$. For a lossy cylinder, its wavenumber k_ℓ is complex, and consequently, q_ℓ is also complex. This motivates the use of the special functions presented in this work to compute the field distributions. The magnetic field is obtained from the electric field using the relation

$$\mathbf{H}(u, v) = H_u(u, v)\hat{\mathbf{u}} + H_v(u, v)\hat{\mathbf{v}} = \frac{i}{\omega\mu d\sqrt{\cosh u^2 \cos v^2}} \left[\hat{\mathbf{u}}\frac{\partial}{\partial v} - \hat{\mathbf{v}}\frac{\partial}{\partial u} \right] E_z(u, v). \tag{69}$$
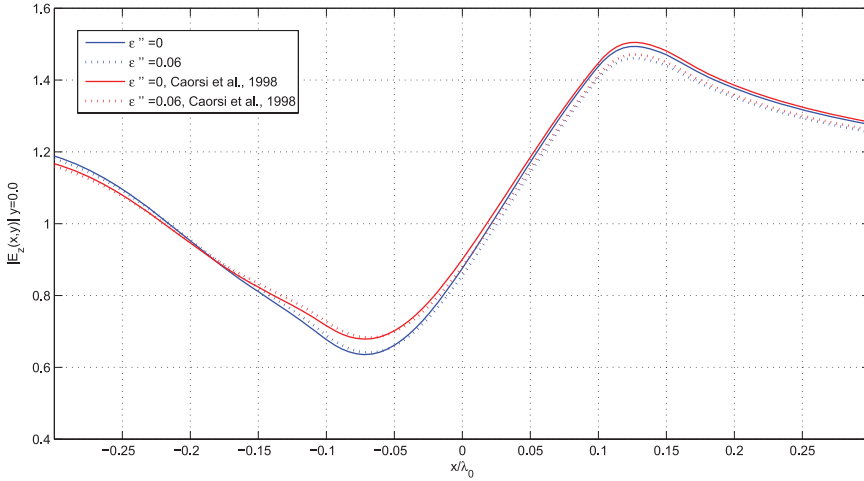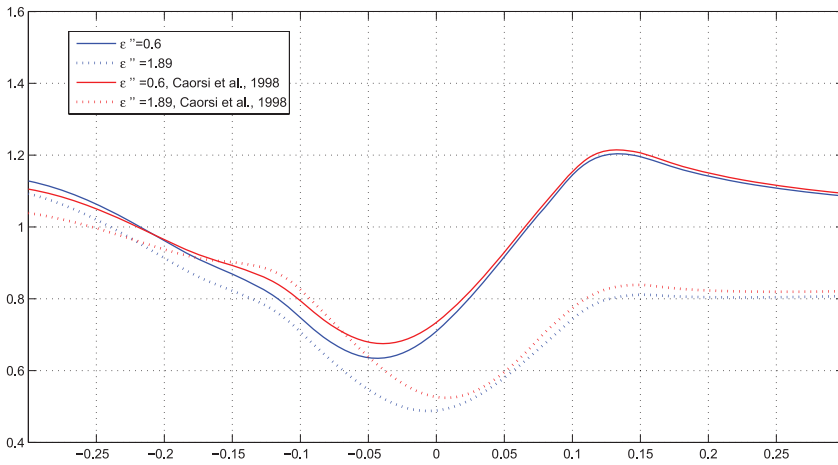
(a) Results for $\epsilon'' = 0$ and $\epsilon'' = 0.06$.

(b) Results for $\epsilon'' = 0.6$ and $\epsilon'' = 1.89$.

Fig. 12.   Magnitudes $|E_z|$ in the four regions of the geometry: comparison between the computation method presented in Caorsi et al. [1998] and the method presented here.

The expansion coefficients $e_{\ell,m}$, $f_{\ell,m}$, $g_{\ell,m}$, $h_{\ell,m}$ are obtained by imposing the electromagnetic boundary conditions on the continuity of the tangential components of the total electric and magnetic fields across the interfaces between different materials.

This approach is similar to, for example, the one for the multilayer circular cylinder. However, in this case it is not possible to explicitly write in closed form, the expansion coefficients of the scattered field in terms of the expansion coefficients of the incident field because the angular Mathieu functions depend on the material properties through the parameter q. This does not happen in the circular cylinder case. It is also worth noting that the orthogonality relations (22)–(23) are not valid across an interface when the material properties change, however they may be used as in, for example

[Caorsi et al. 1997, 1998, 1999b]. Therefore, the point-matching method, which enforces the boundary conditions at predetermined points [Balanis 1989], is used in this work. Let m_{max} be the maximum order of the expansion coefficients, then $N_t = 6m_{max} + 3$ is the total number of uniformly distributed points where the boundary conditions are enforced, as shown in Figure 11(b).

The application of the boundary conditions at each point leads to a system of $12m_{max} + 6$ equations, which is solved by a matrix inversion.

Numerical results are shown in Figure 12 for the electric field computed with the methods presented in Caorsi et al. [1998] and with the method presented in this work. The geometry is the same in all cases, where the semimajor axes of the three layers of the elliptic cylinder have length $u_1 = 0.10\lambda_0$, $u_2 = 0.13\lambda_0$, and $u_3 = 0.16\lambda_0$, and $d = 0.16\lambda_0$. The complex relative dielectric permittivities $\epsilon_i = \epsilon_i' - i\epsilon_i''$ of the three layers are $\epsilon_1' = 1.0$, $\epsilon_2' = 4.0$, $\epsilon_3' = 2.5$, and $\epsilon_1'' = \epsilon_2'' = \epsilon_3'' = \epsilon''$. The solution has been computed for $\epsilon'' = 0$ (pure dielectric cylinder), $\epsilon'' = 0.06$ (weakly lossy cylinder), $\epsilon'' = 0.6$ (lossy cylinder), and $\epsilon'' = 1.89$ (very lossy cylinder).

All results are computed by considering $m_{max} = 9$. For all values of ϵ'' there is good agreement between the methods presented in Caorsi et al. [1998] and the method presented here. The differences between the two results may be attributed to how the boundary conditions are applied and to the computation of the Mathieu functions. Specifically, in Caorsi et al. [1998], the boundary conditions are enforced using the Galerkin method, which is different from the point matching method used in this article. In addition, in Caorsi et al. [1998], the Mathieu functions for complex values of the parameter q are computed using a Taylor series expansion.

7. CONCLUSIONS

This article describes the computation of Mathieu functions for complex values of the parameter q. The associated Fortran 90 software was validate in different ways and a sample problem that requires the use of such functions was provided.

ACKNOWLEDGMENTS

REFERENCES

ABRAMOVITZ, M. AND ANDSTEGUN, I. A. 1970. *Handbook of Mathematical Functions*. Dover Publications, Inc., New York.

AKGOL, O., DANIELE, V., ERRICOLO, D., AND ANDUSLENGHI, P. 2011. Radiation from a line source shielded by a confocal elliptic layer of DNG metamaterial. *IEEE Antennas Wirel. Propag. Lett.* 10, 943–946.

AKGOL, O., ERRICOLO, D., AND USLENGHI, P. 2011a. Electromagnetic radiation and scattering for a gap in a corner backed by a cavity filled with DNG metamaterial. *Radio Sci. 46*, RS4005. doi:10.1029/2010RS004471.

AKGOL, O., ERRICOLO, D., AND USLENGHI, P. 2011b. Exact imaging by an elliptic lens. *IEEE Antennas Wirel. Propag. Lett. 10*, 639–642.

ALHARGAN, F. A. 2001. Algorithms for the computation of all Mathieu functions of integer order. *ACM Trans. Math. Softw. 26*, 3, 390–407.

AMOS, D. E. 1986. Algorithm 644: A portable package for Bessel functions of a complex argument and nonnegative order. *ACM Trans. Math. Softw. 12*, 265–273.

BAKER, L. 1992. *Mathematical Function Handbook*. McGraw-Hill.

BAKKER, M. AND KUHLMAN, K. 2011. Computational issues and applications of line-elements to model subsurface flow governed by the modified Helmholtz equation. *Adv. Water Resources 34*, 9, (Special Issue on New Computational Methods and Software Tools), 1186–1194.

BAKTUR, R., PEARSON, L. W., AND BALLATO, J. 2010. An analysis of coupling between a whispering gallery mode laser in an elliptical microring and the dominant mode in the coaxially oriented elliptical optical fiber. *J. Appl. Physics* 107, 2. DOI: 10.1063/1.3284947.

BALANIS, C. A. 1989. *Advanced Engineering Electromagnetics*. Wiley, New York.

BERARDI, C., ERRICOLO, D., AND USLENGHI , P. 2004. Exact dipole radiation for an oblate spheroidal cavity filled with isorefractive material and aperture-coupled to a half space. *IEEE Trans. Antennas Propag. 52*, 9, 2205–2213.

BLANCH, G. 1966. Numerical aspects of Mathieu eigenvalues. In *Rend. Circ. Mat. Paler. 2 Series*, vol. 15. 51–97.

BLANCH, G. AND CLEMM, D. 1969. *Mathieu's Equation For Complex Parameters. Tables Of Characteristic Values*. Aerospace Research Laboratories.

BLANCH, G. AND RHODES, I. 1955. Tables of characteristic values of Mathieu's equation for large values of the parameter. *J. Washington Acad. Sci. 45*, 6, 166–196.

BOWMAN, J. J., SENIOR, T. B. A., AND USLENGHI, P. L. E. 1987. *Electromagnetic and Acoustic Scattering by Simple Shapes*. Hemisphere Publishing Corporation, New York.

CANTA, S. AND ERRICOLO, D. 2008. Exact 2D scattering analysis of a slot backed by a semielliptical cavity and covered by a multilayer diaphragm. *Radio Sci.* doi:10.1029/2007RS003809.

CAORSI, S., PASTORINO, M., AND M. RAFFETTO. 1997. Electromagnetic scattering by a multilayer elliptic cylinder under transverse-magnetic illumination: Series solution in terms of Mathieu functions. *IEEE Trans. Antennas Propag. 45*, 6, 926–935.

CAORSI, S., PASTORINO, M., AND RAFFETTO, M. 1998. Electromagnetic scattering by weakly lossy multilayer elliptic cylinders. *IEEE Trans. Antennas Propag. 46,* 11, 1750–1751.

CAORSI, S., PASTORINO, M., AND RAFFETTO, M. 1999a. Electromagnetic scattering by a conducting strip with a multilayer elliptic dielectric coating. *IEEE Trans. Electromagn. Compat. 41*, 4, 335–343.

CAORSI, S., PASTORINO, M., AND RAFFETTO, M. 1999b. EM field prediction inside lossy multilayer elliptic cylinders for biological-body modeling and numerical-procedure testing. *IEEE Trans. Biomed. Eng. 46,* 11, 1304–1309.

CLEMM, D. S. 1969. Algorithm 352 Characteristic values and associated solutions of Mathieu's differential equation [S22]. *Comm. ACM 12*, 7, 399–407.

CLEMM, D. S. 1970. Remark on algorithm 352 [S22] Characteristic values and associated solutions of Mathieu's differential equation. *Comm. ACM 13*, 12, 750.

ERRICOLO, D. 2003. Acceleration of the convergence of series containing Mathieu functions using Shanks transformation. *IEEE Antennas Wirel. Propag. Lett. 2*, 58–61.

ERRICOLO, D. 2006. Algorithm 861: Fortran 90 subroutines for computing the expansion coefficients of Mathieu functions using Blanch's algorithm. *ACM Trans. Math. Software 32*, 4, 622–634.

ERRICOLO, D., CANTA, S. M., HAYVACI, H. T., AND ALBANI, M. 2008. Experimental and theoretical validation for the incremental theory of diffraction. *IEEE Trans. Antennas Propag. 56*, 8, 2563–2571.

ERRICOLO, D., LOCKARD, M., BUTLER, C., AND USLENGHI, P. 2005a. Currents on conducting surfaces of a semielliptical-channel-backed slotted screen in an isorefractive environment. *IEEE Trans. Antennas Propag. 53*, 7, 2350–2356.

ERRICOLO, D., LOCKARD, M. D., BUTLER, C. M., AND USLENGHI, P. L. E. 2005b. Numerical analysis of penetration, radiation, and scattering for a 2D slotted semielliptical channel filled with isorefractive material. *PIER 53*, 69–89.

ERRICOLO, D. AND USLENGHI, P. 2005a. Exact radiation for dipoles on metallic spheroids at the interface between isorefractive half-spaces. *IEEE Trans. Antennas Propag. 53*, 12, 3974–3981.

ERRICOLO, D., USLENGHI, P., ELNOUR, B., AND MIOC, F. 2006. Scattering by a blade on a metallic plane. *Electromagnetics 26*, 1, 57–71.

ERRICOLO, D. AND USLENGHI, P. L. E. 2004. Exact radiation and scattering for an elliptic metal cylinder at the interface between isorefractive half-spaces. *IEEE Trans. Antennas Propag. 52*, 9, 2214–2225.

ERRICOLO, D. AND USLENGHI, P. L. E. 2005b. Penetration, radiation, and scattering for a cavity-backed gap in a corner. *IEEE Trans. Antennas Propag. 53*, 8, 2738–2748.

FRISCH, M. J. 1972. Remark on algorithm 352 [S22] Characteristic values and associated solutions of Mathieu's differential equation. *Comm. ACM 15,* 12, 1074.

GIL, A., SEGURA, J., AND TEMME, N. 2011. Basic methods for computing special functions. In *Recent Advances in Computational and Applied Mathematics*, T. E. Simos, Ed., Springer, 67–121.

GUPTA, S., POULIKAKOS, D., AND KURTCUOGLU, V. 2008. Analytical solution for pulsatile viscous flow in a straight elliptic annulus and application to the motion of the cerebrospinal fluid. *Physics of Fluids 20*, 9. DOI: 10.1063/1.2988858.

HODGE, D. B. 1972. The calculation of the eigenvalues and eigenvectors of Mathieus equation. NASA contractor report, The Ohio State University, Columbus, OH.

IMSL 1994. *IMSL Fortran Subroutines for Mathematical Applications*. Visual Numerics, Inc.

LARSEN, T., ERRICOLO, D., AND USLENGHI, P. 2008. New method to obtain small parameter power series expansions of Mathieu radial and angular functions. *Math. Comput. 87*, 255–274.

MATHIEU, E. L. 1868. Memoire sur le mouvement vibratoire d'une membrane de forme elliptique. *Jour. de Math. Pures et Appliquées (Jour. de Liouville) 13*, 137–203.

MCLACHLAN, N. W. 1964. *Theory and Application of Mathieu Functions*. Dover Publications, New York.

MEIXNER, J. AND SCHAFKE, F. W. 1954. *Mathieusche Funktionen und Sphäroidfunktionen.* Springer, Berlin.

MOON, P. AND SPENCER, D. 1961. *Field Theory Handbook Including Coordinate Systems Differential Equations and Their Solutions*. Springer.

NATIONAL BUREAU OF STANDARDS. 1951. *Tables Relating to Mathieu Functions*. Columbia University Press, New York.

OLSHANSKY, Y. AND TURKEL, E. 2008. The inverse problem of an impenetrable sound-hard body in acoustic scattering. *J. Physics: Conference Series 135*, 1, 012079.

RENGARAJAN, S. R. AND LEWIS, J. 1980. Mathieu functions of integraf orders and real arguments. *IEEE Trans. Microw. Theory Tech. 28*, 3, 276–277.

SHIRTS, R. B. 1993a. Algorithm 721 MTIEU1 and MTIEU2: Two subroutines to compute eigenvalues and solutions to Mathieu's differential equation for noninteger order. *ACM Trans. Math. Softw. 19*, 3, 391–406.

SHIRTS, R. B. 1993b. The computation of eigenvalues and solutions of Mathieu's differential equation for noninteger order. *ACM Trans. Math. Softw. 19*, 3, 377–390.

STAFF OF THE COMPUTATION LABORATORY. 1967. *Tables Relating to Mathieu Functions* 2nd Ed. Applied Mathematics Series. U.S. Government Printing Office, Washington, D.C.

STRATTON, J. A. 1941. *Electromagnetic Theory.* McGraw-Hill, New York.

VALENTINO, M. AND ERRICOLO, D. 2006. Exact two-dimensional scattering from a slot in a ground plane backed by a semielliptical cavity and covered with an isorefractive diaphragm. *Radio Sci. 42*, RS6S12. doi:10.1029/2006RS003547.

VALENTINO, M. AND ERRICOLO, D. 2007. Exact radiation of a dipole in the presence of a circular aperture in a ground plane backed by a spheroidal cavity and covered with an isorefractive diaphragm. *Radio Sci. 42*. RS6S13, doi:10.1029/2006RS003548.

WOLFRAM, S. 2003. *The Mathematica® Book* 5th Ed. Wolfram Media.

ZHANG, S. AND JIN, J.-M. 1996. *Computation of Special Functions.* Wiley, New York.